Journal of Applied Electrochemistry (2005) 35:1067–1072
DOI 10.1007/s10800-005-9002-1

Comparison of the characteristics of electric double-layer capacitors with an activated carbon powder and an activated carbon fiber

ICHIRO TANAHASHI
Department of Applied Chemistry, Faculty of Engineering, Osaka Institute of Technology, 5-16-1 Omiya, Asahi-ku, Osaka 535-8585, Japan (e-mail: tanahashi@chem.oit.ac.jp)

Received 21 February 2005; accepted in revised form 1 June 2005

Key words: activated carbon, capacitor, electric double-layer, pore size distribution, surface area

Abstract

The characteristics of electric double-layer capacitors (EDLCs) with activated carbon powder (ACP), pulverized activated carbon fiber (ACF), and ACF-cloth have been compared. The BET surface areas of the ACP and ACF were estimated to be 1740 and 1970 $m^2\ g^{-1}$, respectively. In the pore-size distribution curve of the ACP and ACF, the most dominant pore diameter was 1.8 and 1.1 nm for the ACP and ACF, respectively. Disc- and cloth-type of electrodes were fabricated using ACP and ACF. The electrical resistance of the ACF-disc and ACF-cloth electrodes was four orders of magnitudes lower than that of the ACP-disc electrodes. In accordance with the lower electrical resistance of the ACF-disc and ACF-cloth, the d.c. resistance of the EDLC with the ACF-disc and with ACF-cloth was lower than that of the EDLC with the ACP-disc. The highest specific volume capacitance of 28.3 F cm^{-3} (capacitance / volume of total ACF in the EDLC) was achieved with the ACF-disc. In the cyclic voltammograms of the ACF-disc, the stable electric double-layer charging and discharging behavior was observed.

1. Introduction

Electric double-layer capacitors (EDLCs) have been widely used as energy storage devices for memory back-up systems and are expected to be applicable as startup devices for hybrid cars [1]. The energy storage mechanism of EDLCs is based on the phenomenon that an electric double-layer is formed at the boundary between an electrode and an electrolyte. In electronic devices requiring higher discharge currents and smaller size, the lower d.c. resistance of the EDLCs with higher specific volume capacitances becomes an important factor in achieving high performance.

Activated carbons are usually used for EDLC electrodes because of their large specific surface area and high electrical conductivity. In recent years, various types of activated carbons such as an activated carbon powder (ACP) [2], an activated carbon fiber cloth (ACF-cloth) [3–6] and a synthetic carbon aerogel [7] have been investigated in an attempt to develop high-performance EDLCs.

It is known that the characteristics of EDLCs, such as the capacitance and d.c. resistance are largely influenced by the specific surface area and pore size distribution [8]. The characteristics of EDLCs are also influenced not only by the shape of the activated carbon itself but also by the shape of the electrode; disc, cloth or sheet. ACF-cloth electrodes [9–12] show high EDLC performance in comparison with other kinds of activated carbons, because the ACF-cloth has a high specific surface area and suitable pore size distribution for forming an electric double-layer. Moreover, the ACF-cloth is a self-supported material; therefore binders, which are usually insulators, are not necessary to prepare the EDLC electrodes. Thus, the ACF-cloth electrode without binder shows the highest electrical conductivity. However, one of the weak points of the ACF-cloth electrode is its low bulk density, which makes the EDLC large. On the other hand ACPs are widely used as EDLC electrodes. However, the electrical resistance of ACP electrodes is high because the electrodes contain more than 10 wt% of binders such as poly tetrafluoroethylene (PTFE). In order to reduce the electrical resistance of the ACP electrodes, conductive materials such as carbon blacks (CBs) are necessary to mix in the electrodes.

In this paper, we report on the characterization of ACP and ACF and the comparison of EDLC characteristics with four kinds of electrodes; (a) disc-type electrode with ACP (ACP-disc), (b) disc-type one with

ACP and CB ((ACP + CB)-disc), (c) disc-type one with pulverized ACF (ACF-disc) and (d) cloth-type electrode of ACF-cloth.

2. Experimental

2.1. *Preparation of electrodes*

Four kinds of electrodes were fabricated using ACP (Wako Chemical Co. Ltd., Lot. No. SEE0372), ACF-cloth (Nippon Kynol Inc.) and CB (Ketjenblack International Corporation, Ketjenblack). The ACP-disc was prepared from the ACP and PTFE dispersion (Daikin Industries, Ltd., D-1E) as a binder in a 30:1 weight ratio, the (ACP + CB)-disc was from the ACP, CB, and PTFE dispersion in a 30:3:1 weight ratio, the ACF-disc was from the pulverized ACF-cloth and PTFE dispersion in a 30:1 weight ratio and the ACF-cloth was used without further treatment. Both the disc- and cloth-type electrodes were 6.0 mm in diameter and dried for more than 12 h at 100 °C before constructing the EDLCs. The disc-type electrodes were fabricated as follows; the mixtures of ACP + PTFE dispersion, ACP + CB + PTFE dispersion and pulverized ACF + PTFE dispersion were respectively densified into discs in molds applying a pressure of 34.6 MPa by using a steel mold-type pressure apparatus. Physical properties of the four kinds of electrode are listed in Table 1.

Two-electrode EDLC cells were prepared to examine the performances of the EDLC with four kinds of electrodes. The electrodes were attached to stainless steel (SUS304) plates (thickness: 0.35 mm) serving as the collector electrode by conducting carbon paint (Acheson Japan Ltd, Electrodag 502). Two sheets of paper (Nippon Kodoshi Co., VL-120) made of natural pulp were used as the separator to prevent short circuit. The cells were fabricated with two facing electrodes, and the separator was sandwiched between two electrodes. The assembly was housed using a pair of acrylic acid resin plates (5 mm in thickness) with a hole at all the corners and fixed tightly with the acrylic acid resin screws at all the corners. 5.35 M aqueous solution of KOH was used as electrolyte.

2.2. *Material characterization*

The specific surface area and pore size distribution of ACP and ACF was obtained by analyzing the adsorption isotherms of nitrogen at 77 K with the well known BET-method and Dollimore-Heal (DH)-method [13].

Table 1. Physical properties of the four kinds of electrode

Electrodes	Density (g cm^{-3})	Thickness (mm)	Resistance (Ω)
ACP-disc	0.38	0.57	222.47
(ACP + CB)-disc	0.38	0.64	0.22
ACF-disc	0.61	0.35	0.05
ACF-cloth	0.20	0.50	0.06

Adsorption experiments were carried out in a commercial volumetric apparatus from BELSORP36 (BEL JAPAN, Inc.) equipped with a high-precision Baratron capacitance manometer. Before the adsorption experiments, the samples were out-gassed at 423 K for 2 h.

The electrical resistance of the mixture of ACP + CB and the four kinds of electrodes was measured according to the JIS (Japan Industrial Standard) K-3054 method using the apparatus shown in Figure 1. About 40 mg of electrode samples was put into the mold (13 mm in diameter) made of phenol resin and pressed by using nickel-plated steel blocks at pressure ranges of 1.73–6.92 MPa at room temperature. The electrical resistance of the samples was estimated by the voltage difference cased by the samples and the current in the circuit shown in Fig. 1 using Ohm's law. The power source and the standard resistance in the circuit shown in the figure were 1.500 V d.c. and 100 Ω, respectively.

The morphology of ACP, pulverized ACF and ACF-cloth was examined by scanning electron microscopy (SEM). The crystallinity of ACP and ACF was characterized by X-ray diffraction (XRD) using a Rigaku RINT 2000 diffractometer with Cu Kα radiation.

2.3. *Electrochemical measurements*

The capacitance measurements of EDLCs were performed with a symmetrical cell configuration (a two-electrode system) by a constant voltage charge and constant current discharge method. The EDLCs were charged at 1.0 V d.c. for more than 30 min, and the specific weight capacitance, C_w, was calculated from the equation, $C_w = it/m\Delta V$, where i is the constant discharge current of 1 mA, t the time for discharge, m the total weight of electrodes in the EDLC, and ΔV the potential change of the EDLC from 0.5 to 0.25 V caused by discharge. The specific volume capacitance, C_v, was calculated from the equation, $C_v = it/v\Delta V$, where v is the total volume of the electrodes in the EDLC. The d.c. resistance, R, of the EDLC was estimated by the voltage drop (IR drop) at the beginning of discharge of the

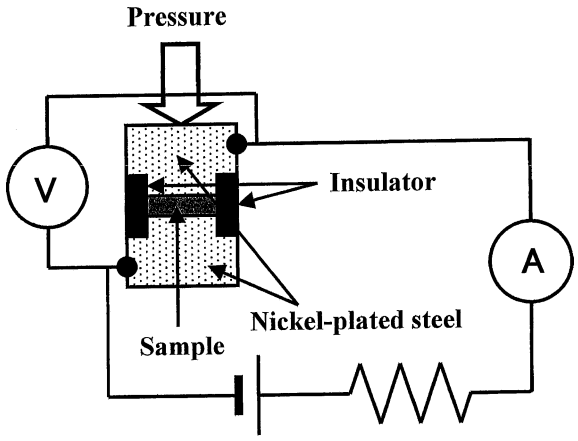

Fig. 1. Cross sectional view of the mold and schematic diagram of the electrical resistance measurement apparatus.

EDLC from the equation, $R = V_{drop}/i$, where V_{drop} is the IR drop and i the constant discharge current of 1 mA. Triangular voltage-sweep cyclic voltammetric measurements were performed in the voltage range from −0.5 to 0.5 V applied between the two electrodes. The potential scan rate was 5.0 mV s^{-1}. The measurement was carried out using a potentiostat (Hokuto Denko, Model HA-303) and a function generator (Hokuto Denko, Model HB-104) at room temperature. All the electrochemical measurements were conducted in an ambient environment by soaking the EDLC cells in the KOH solution in a beaker.

3. Results and discussion

3.1. *Physical characterization of electrodes*

Typical N_2 adsorption-desorption isotherms at 77 K obtained with ACP and ACF are shown in Figure 2(a) and (b), respectively. The isotherm of ACP in Figure 2(a) belongs to type II of the isotherm classification of IUPAC [14]. The isotherm shows a steep rise at low relative pressure is followed by a gradual increase at higher pressure. In addition, a hysteresis loop is observed indicating that the ACP contains a considerable amount of micropores as well as mesopores having an ink-bottle shape. On the other hand, the isotherm of ACF in Figure 2(b) is classified as typical type I containing mainly micropores and the hysteresis of the isotherm is not observed. The slope of the plateau region is probably attributable to additional adsorption on the external surface of the ACF. From the isotherms, the BET surface areas, S_{BET}, of the ACP and ACF were estimated to be 1740 and 1970 $m^2\ g^{-1}$, respectively. The S_{BET} of the ACF was calculated to be 1.13 times larger than that of the ACP. The pore-size distribution of the ACP and ACF was estimated by the N_2 desorption isotherm using D-H method. In the case of the ACP, the maximum of $\Delta V_p/\Delta R_p$ (the differential value of V_p/R_p;R_p: the micropore radius, V_p: the pore volume.) was located at $R_p = 0.9$ nm. Assuming that the walls of pores are parallel plates, we conclude that the most dominant pore diameter of the ACP was 1.8 nm and that of the ACF was 1.1 nm. The ACF shows larger S_{BET} and smaller pore size in comparison with those of the ACP.

SEM photographs of the ACP, pulverized ACF and ACF-cloth are shown in Figure 3(a), (b) and (c), respectively. The ACP is the mixture of large particles with diameters up to 10 μm and small particles with

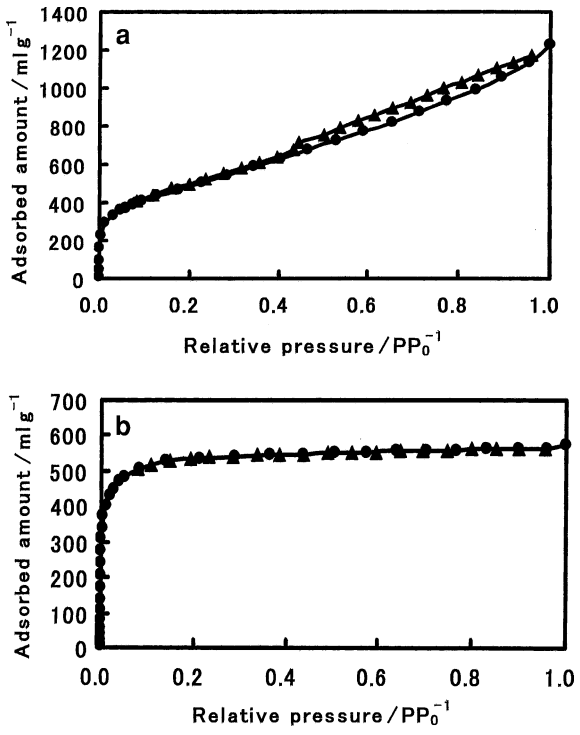

Fig. 2. Nitrogen adsorption–desorption isotherms for (a) ACP and (b) ACF-cloth. ●: adsorption, ▲: desorption.

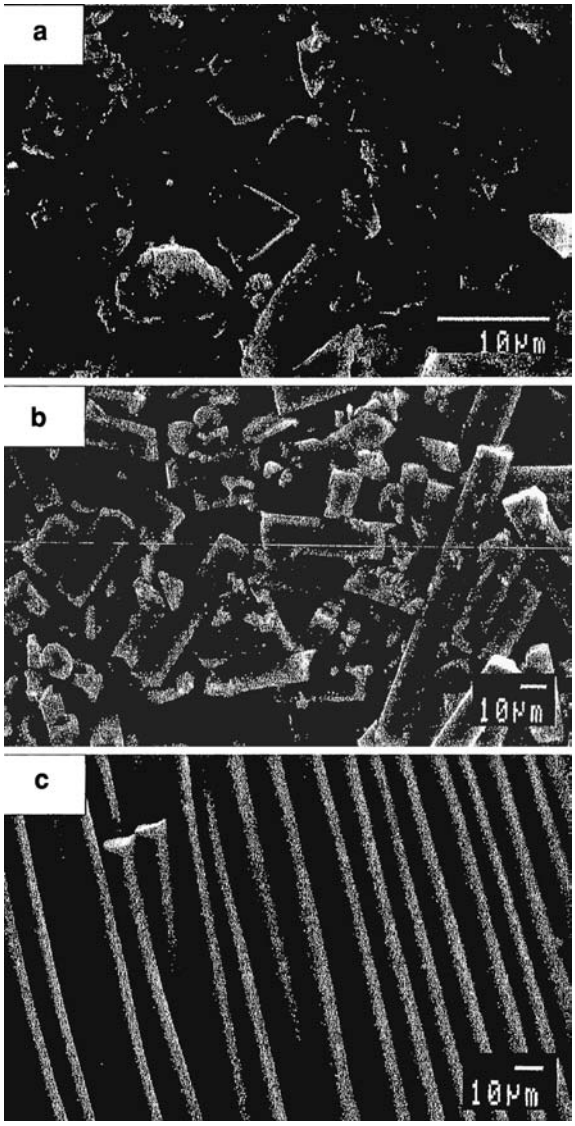

Fig. 3. SEM images for (a) ACP, (b) pulverized ACF-cloth, and (c) ACF-cloth.

diameters less than 1–2 μm and a fracture surface is observed for the large particles shown in Figure 3(a). The pulverized ACF was prepared by grinding the ACF-cloth in a porcelain mortar with a pestle. In Figure 3(b), a part of the fibers are completely pulverized; however most of the pulverized ACF maintains the shape of fiber. Figure 3(c) shows a part of the ACF-cloth. The ACF-cloth was woven with threads which are composed of many fibers with a diameter of 11 μm. From the figure, the density of the ACF-cloth seems to be high. However, the woven ACF-cloth has spaces in its structure; thus the density of the ACF-cloth is low compared with that of disc-type electrodes.

From XRD patterns of ACP and ACF, only the broad peak around 25° was observed, indicating that the ACP and ACF had an amorphous structure. Therefore, intercalation reactions are difficult in the amorphous carbons (ACP and ACF) and aqueous electrolyte KOH systems.

The content of binders in the electrodes affects the electrical resistance of the electrodes. In this experiments, obtaining the electrodes with sufficient mechanical strength to construct the capacitors and with lower electrical resistance, the binder content of ca. 1/30 in the electrodes was optimized. Figure 4 shows the relation between the electrical resistance of the mixture of ACP and CB and the amount of added CB (wt%) to the mixture. The resistance was measured by changing the applied pressure using the apparatus shown in Figure 1. The resistance of the ACP without CB (0 wt%) is more than 200 Ω at a pressure of 1.73 MPa and it decreases with increasing amount of CB. For the mixture containing CB up to 10 wt % the resistance decreased by two orders of magnitudes in comparison with that of the ACP without CB. Thus, the CB is an effective material to reduce the contact resistance of ACP. In the figure, the applied pressure dependence of the resistance is large. This is due to the packing density becoming high and the contact resistance of the mixture becoming lower with increasing applied pressure.

Figure 5 shows the electrical resistance of the four kinds of EDLC electrodes, (a) ACP-disc, (b) (ACP + CB)-disc, (c) ACF-disc and (d) ACF-cloth, at various applied pressures using the apparatus shown in Figure 1. Comparing the Figures 4 and 5, the electrical resistance of (a) ACP-disc and (b) (ACP + CB)-disc is slightly higher than

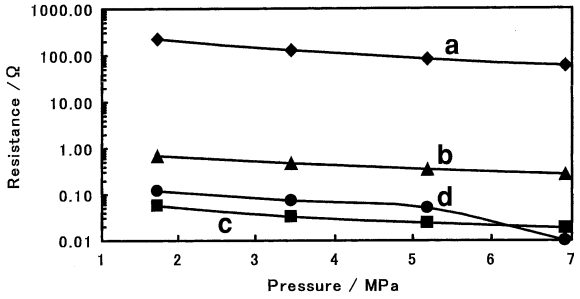

Fig. 5. Relation between the electrical resistance of the four kinds of electrode and the applied pressure. (a) ACP-disc, (b) (ACP + CB)-disc, (c) ACF-disc, and (d) ACF-cloth.

that of the ACP itself (CB: 0%) and the mixture of ACP + CB (10%), respectively. This is due to that the insulating PTFE being necessary as a binder in the case of the disc-type electrodes. Using the PTFE, the electrical resistance of (a) and (b) electrodes became high, however, the mechanical strength of the electrodes increased. The resistances of (a), (b), (c) and (d) electrodes measured at 6.92 MPa are listed in Table 1. The resistances of (c) and (d) electrodes with ACF decreased by four orders of magnitudes in comparison with those of (a) electrode with ACP. In the case of the electrodes with ACF, the conductive paths of fibers exist in the electrodes. Thus the resistances of (c) and (d) electrodes without CB are lower than those of (a) and (b). In Figure 5, the resistance of (d) ACF-cloth becomes lower than that of (c) ACP-disc when the pressure increases at 6.92 MPa. This is because (d) ACF-cloth without binder was pulverized and the packing density became high and contact resistance became low at the pressure.

3.2. *Electrochemical measurement of EDLC*

The conductivity of 5.35 M KOH is one order of magnitude higher than that of organic solutions of alkyl ammonium salts and the electrochemical reactivity between stainless steel plates as metal collector electrodes and KOH solutions is low, thus the aqueous solution of KOH was used as electrolytes. Figure 6 shows typical discharge curves of the four kinds of EDLCs, (A) EDLC with ACP-disc, (B) one with

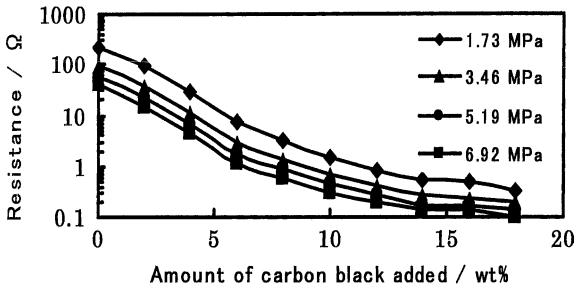

Fig. 4. Relation between the electrical resistance of the mixture of ACP and CB and the amount of CB added (wt %) at various pressures.

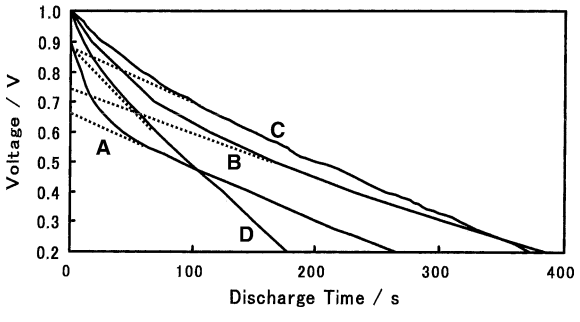

Fig. 6. Typical discharge curves of (A) EDLC with ACP-disc, (B) EDLC with (ACP + CB)-disc, (C) EDLC with ACF-disc, and (D) EDLC with ACF-cloth.

(ACP + CB)-disc, (C) one with ACF-disc, and (D) one with ACF-cloth, after charging the EDLCs at constant 1.0 V d.c. for more than 30 min. The discharge current was constant 1 mA. The curves are typical of the discharge performance of an EDLC. In the figure, the voltage drops at the beginning of discharge are steep. In these curves, the IR drop could not be estimated clearly. Thus, extrapolating the straight part of the discharge curves to the vertical axis shown by the dotted lines in the figure, and the voltage difference between 1.0 V and the voltage of the extrapolating line at discharge time of 0 s was regarded as the IR drop. Although the capacitance of the EDLCs was different from capacitor to capacitor, the IR drop of (A) and (B) EDLCs is higher than that of (C) and (D) EDLCs. From the values of IR drop, the d.c. resistances, R, of EDLCs were calculated and are listed in Table 2. The IR drop of EDLCs was caused by different kinds of electrical resistance inside the EDLC, such as the resistance of electrodes, electrolytes, and contact resistance. In accordance with the lower resistance of ACF-disc and ACF-cloth, the (C) and (D) EDLCs showed the lower d.c. resistances listed in Table 2. The IR drop is largely affected by the resistance of the electrodes. The IR drop is also affected by the discharge rate. However, the rate capability of the capacitors did not examine in this experiments. Further investigation is necessary to clarify the rate dependence of the IR drops. In Table 2, C_w of EDLCs is comparable for all kinds of electrode. The S_{BET} of ACP was lower in comparison with that of ACF, however, the pore size of ACP was larger than that of ACF. Thus, in the case of (B) EDLC with (ACP + CB)-disc, an electric double-layer seems to be effectively formed at the interface between the ACP and the electrolyte. Because of the difference in pore size distribution between the ACP and ACF, the C_w was not proportional to the S_{BET} of the ACP and ACF. However, the C_v of EDLCs depended largely on the type of electrode. The highest C_v of 28.3 F cm^{-3} (capacitance/total volume of electrodes in the EDLC) was achieved with the ACF-disc. The C_v of (D) EDLC with ACF-cloth is under a half of that of other EDLCs. This is because that the ACF-cloth showed the lowest packing density in the four kinds of electrode listed in Table 1. On the other hand, the density of the ACF-disc was more than three times as high as that of the ACF-cloth.

Cyclic voltammetry is a helpful measurement in understanding electrochemical behavior of EDLCs during the charge and discharge process. The cyclic voltammogram of an ideal EDLC must be a regular square shape, while that of the non-ideal EDLC with distributed capacity and/or Faradaic processes becomes a parallelogram shape [15, 16]. Distributed capacity effects arise when the exterior surface of the porous electrode charges or discharges faster than that the interior and when the resistance of the electrode is not uniform. An increase in the resistance of the electrolyte in the pores of the electrode enhances this effect. Figure 7 shows the cyclic voltammograms (CVs) of above-mentioned (A), (B), (C), and (D) EDLCs. In Figure 7, the CV of (A) EDLC with ACP-disc shows a parallelogram shape indicating that the distributed capacity effects are large. This is probably due to the contact resistance of ACP-disc being large and the uniformity of the ACP being low as shown in Figure 3(a). In the CVs of (B), (C), and (D), the distributed capacity effects become small in comparison with that of (A). This indicates that the electric double-layer charging and discharging behavior is influenced by the electrical resistance of the electrodes.

Table 2. Characteristics of the EDLCs with four kinds of electrode

Electrodes	Specific weight capacitance: C_w(F g^{-1})	Specific volume capacitance: C_v(F cm^{-3})	D.C. resistance: R(Ω)
ACP-disc	47.2	17.9	344
(ACP + CB)-disc	49.9	19.0	252
ACF-disc	46.3	28.3	132
(ACF-cloth)	48.0	9.3	120

4. Conclusions

The N_2 adsorption–desorption isotherm of ACP and ACF belong to type II and type I of the isotherm classification of IUPAC, respectively. The S_{BET} of the ACF (1970 m^2 g^{-1}) with the most popular pore diameter of 1.1 nm was calculated to be 1.13 times larger than that of the ACP (1740 m^2 g^{-1}) with the most dominant pore diameter of 1.8 nm. The electrical resistance of the ACF-disc and ACF-cloth was lower than that of the ACP-disc. In accordance with the lower electrical resistance of the electrodes with ACF, the d.c. resistance of the EDLC with the ACF-disc and with ACF-cloth was lower than that of the EDLC with the ACP-disc and with (ACP + CB)-disc. The density of the ACF-disc was more than three times as high as that of the ACF-cloth. Therefore, the highest specific volume capacitance of 28.3 F cm^{-3} was achieved with the ACF-disc and showed a stable electric double-layer charging and discharging behavior. The ACF-disc is a suitable electrode for EDLCs.

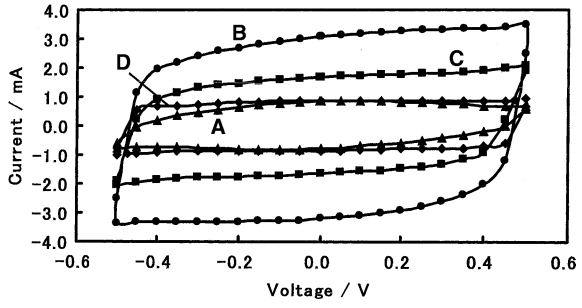

Fig. 7. Cyclic voltamograms of the four kinds of EDLCs at 5 mV s^{-1}. ▲: (A) EDLC with ACP-disc, ●: (B) EDLC with (ACP + CB)-disc, ■: (C) EDLC with ACF-disc, and ◆: (D) EDLC with ACF-cloth.

References

1. M. Okamura, H. Hasuike, M. Yamagishi and S. Araki, *Electrochemistry* **69** (2001) 414.
2. R. Asakura, T. Kondo, M. Morita, H. Hatori and Y. Yamada, *TANSO* **No. 215** (2004) 231.
3. H. Nagasawa, A. Shudo and K. Miura, *J. Electrochem. Soc.* **147** (2000) 38.
4. Y.O. Choi, K.S. Yang and J.H. Kim, *Electrochemistry* **69** (2001) 837.
5. S. Shiraishi, H. Kurihara and A. Oya, *Electrochemistry* **69** (2001) 440.
6. S.R. Hwang and H. Teng, *J. Electrochem. Soc.* **149** (2002) A591.
7. S.T. Mayer, R.W. Pekala and J.L. Kaschmitter, *J. Electrochem. Soc.* **140** (1993) 446.
8. M. Endo, T. Maeda, T. Takeda, Y.J. Kim, K. Koshiba, H. Hara and M.S. Dresselhaus, *J. Electrochem. Soc.* **148** (2001) A910.
9. I. Tanahashi, A. Yoshida and A. Nishino, *Denki Kagaku (Electrochemistry)* **56** (1988) 892.
10. I. Tanahashi, A. Yoshida and A. Nishino, *J. Electrochem. Soc.* **137** (1990) 3052.
11. I. Tanahashi, A. Yoshida and A. Nishino, *Carbon* **29** (1991) 1033.
12. I. Tanahashi, A. Yoshida and A. Nishino, *J. Appl. Electrochem.* **21** (1991) 28.
13. D. Dollimore and G.R. Heal, *J. Appl. Chem. Soc.* **14** (1964) 109.
14. K.S.W. Sing, *Pure Appl. Chem.* **57** (1985) 603.
15. E.G. Gagnon, *J. Electrochem. Soc.* **122** (1975) 521.
16. J. Koresh and A. Soffer, *J. Electrochem. Soc.* **124** (1977) 1379.